jmr&t
Journal of Materials Research and Technology
www.jmrt.com.br

Original Article

Passivation behavior of a ferritic stainless steel in concentrated alkaline solutions

*Arash Fattah-alhosseini**, *Saeed Vafaeian*

Department of Materials Engineering, Bu-Ali Sina University, Hamedan, Iran

ARTICLE INFO

Article history:
Received 18 June 2014
Accepted 4 February 2015
Available online 12 March 2015

Keywords:
Alkaline solution
Ferritic stainless steel
Mott–Schottky
Donor density

ABSTRACT

The passivation behavior of AISI 430 ferritic stainless steel was investigated in concentrated alkaline solutions in relation to several test parameters, using electrochemical techniques. Increasing solution pH (varying from 11.5 to 14.0) leads to an increase in the corrosion rate of the alloy. Mott–Schottky analysis revealed that passive films formed on AISI 430 ferritic stainless steel behave as n-type semiconductor and the donor densities increased with pH. Electrochemical impedance spectroscopy (EIS) results showed that the reciprocal capacitance of the passive film is directly proportional to its thickness, which decreases with pH increase. The results revealed that for this ferritic stainless steel in concentrated alkaline solutions, decreasing the solution pH offers better conditions for forming passive films with higher protection behavior, due to the growth of a much thicker and less defective film.

1. Introduction

Proton exchange membrane fuel cell (PEMFC) has widely attracted an attention. Bipolar plates are important components in PEMFC and stainless steel is popularly used as bipolar plate material. In the recent years, many studies on stainless steel bipolar plate material have been on austenitic steels [1–5]. Also, there were some works on the effects of various factors such as acidity, fluoride ions, temperature and polarization potential on the corrosion behavior of the austenitic stainless steel bipolar plates [6–10].

Former investigations showed that the effectiveness of the austenitic stainless steels determined by the quantity of Cr, with higher Cr leading to better behavior [6–9]. However, austenitic stainless steels have a high Ni content, which increases their cost. Generally, former works on the nature of the passive film formed on austenitic stainless steels revealed that Ni is not a major component of it. This indicates that Ni could be eliminated without changing the passivation effectiveness [5]. Also, Wind et al. [11] reported that Ni from AISI 316L austenitic stainless steel can be a major contaminant in the membrane, reducing the total conductivity. Thus far, there has been very little research on ferritic stainless steels,

* *Corresponding author.*
E-mail: a.fattah@basu.ac.ir (A. Fattah-alhosseini).
http://dx.doi.org/10.1016/j.jmrt.2015.02.003

which have low or no Ni but similar Cr contents. Therefore, the selection of a ferritic stainless steel was chosen for this work.

In the polymer electrolyte membrane fuel cell, the interfacial contact resistance is influenced by the material property, surface topology, operation condition and the property of the passive film such as the composition and thickness [12]. Of late, there have been several methods to modify the property of the passive film (such as the electrochemical surface treatment [13] and the addition of the alloying element [14]). Moreover, the immersion in the alkaline solution is one of the useful methods to improve the properties of the passive film. In NaOH solutions, the passive film transforms from iron oxide-rich film to passive film enriched with chromium oxide and depleted in iron oxide [12,15].

Generally, increasing research on the electronic properties of passive films formed on stainless steels has given an important contribution to the understanding of the corrosion behavior of these alloys. In practice, the passive film composition varies with the solution pH used for film formation and this is expected to affect the semiconducting properties of the passive film [16,17]. According to the point defect model (PDM) [18–20], the growth of the passive film involves the migration of these point defects under the influence of the electrostatic field in the film. Thus, the key parameters in determining the transport of point defects and hence the kinetics of film growth is the density and the diffusivity of the defects in film. In the last decade, by employing the Mott–Schottky analysis in conjunction with the PDM, the point defects density and diffusivity for some metals and alloys have been determined [18–20].

In this work, the EIS and Mott–Schottky analysis of AISI 430 ferritic stainless steel in NaOH solutions at open circuit potential (OCP) was performed and the passivation parameters and defects concentrations were calculated as a function of pH solution. Also, the relationship between the donor density and pH solution are discussed in order to understand the passivation characteristics of AISI 430 ferritic stainless steel.

2. Experimental procedures

The chemical composition of AISI 430 ferritic stainless steel is shown in Table 1. All samples were ground to 2000 grit and cleaned with distilled water prior to tests. Aerated alkaline solutions (without purging oxygen or any gas) with NaOH and distilled water were prepared at different pH (11.5, 12.0, 12.5, 13.0, 13.5, and 14.0).

The electrochemical measurements were performed in the following sequence:

(a) Potentiodynamic polarization curves were measured potentiodynamically at a scan rate of 1 mV s^{-1} starting from −0.25 V (vs. OCP).
(b) EIS test at OCP DC potential with AC potential perturbation amplitude of 10 mV and frequency range of 100 kHz to 10 mHz.
(c) Mott–Schottky analysis was carried out on the passive films at a frequency of 1 kHz using a 10 mV ac signal and a step potential of 25 mV, in the cathodic direction.

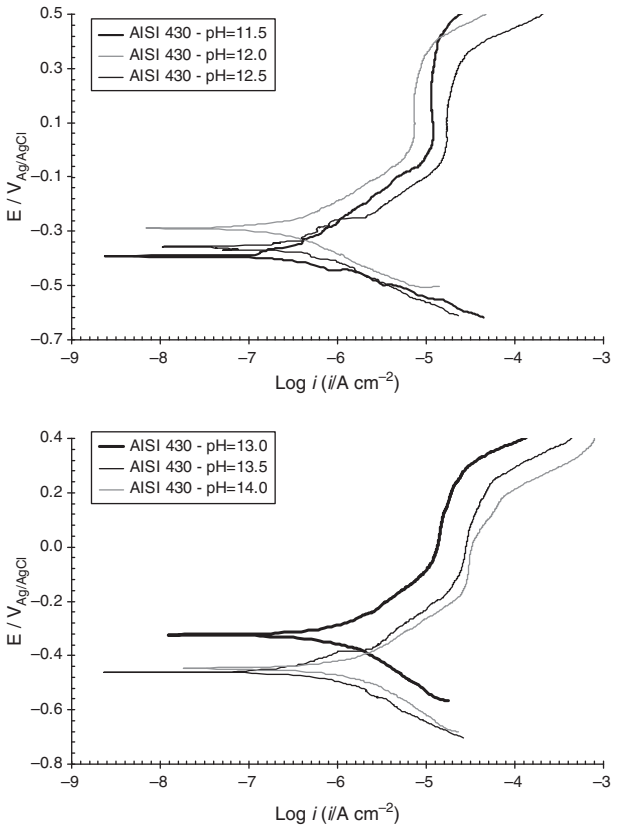

Fig. 1 – Potentiodynamic polarization curves of AISI 430 stainless steel in NaOH solutions with pH varying from 11.5 to 14.0.

Before all electrochemical tests, the working electrodes were immersed in the investigated solutions at OCP to form a steady-state passive film. All electrochemical measurements were performed in a conventional three-electrode flat cell. The counter electrode was a Pt plate, and all potentials were measured against Ag/AgCl in saturated KCl. All electrochemical measurements were obtained using Autolab potentiostat/galvanostat controlled by a personal computer. For the EIS data modeling and curve-fitting method, the NOVA impedance software was used.

3. Results and discussion

3.1. *Potentiodynamic polarization measurements*

Fig. 1 shows the potentiodynamic polarization curves of AISI 430 ferritic stainless steel in NaOH solutions with pH varying from 11.5 to 14.0. By comparing the polarization curves for this stainless steel in different pH solutions, the current density was found to increase with potential during the low polarization range and no obvious current peak was observed. Also, all curves exhibit similar features, with a broad passive range up to the onset of transpassivity.

Tafel extrapolation method is widely used for the measurement of the corrosion rate. By this method, the corrosion current density (i_{corr}) was calculated of the linear part for the

Table 1 – Chemical composition of AISI 430 ferritic stainless steel.

	Cr	Ni	Mo	Mn	Si	C	P	Cu	N	Co	Fe
AISI 430/wt%	16.50	0.13	0.02	0.53	0.50	0.05	0.025	0.07	0.06	0.02	Bal

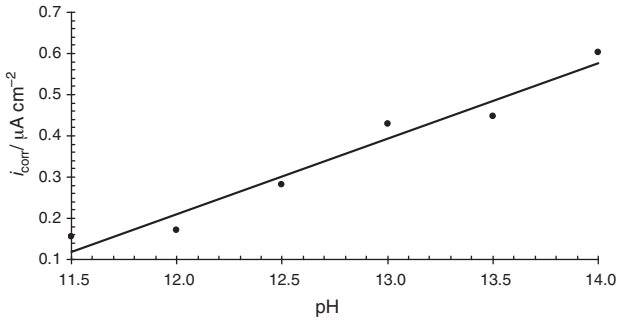

Fig. 2 – Effect of solution pH on the corrosion current density of AISI 430 stainless steel.

cathodic branch back to the mixed potential of zero net current (E_{corr}) with accuracy of more than 95% for the points more negative to E_{corr} by 50 mV [21–23]. Fig. 2 shows the effect of solution pH on the corrosion current density of AISI 430 stainless steel. It is evident from this figure that the corrosion current density increased linearly with pH.

3.2. *Mott–Schottky analysis*

Fig. 3 shows the Mott–Schottky plots of AISI 430 ferritic stainless steel in NaOH solutions with pH varying from 11.5 to 14.0. It should be noted that for this stainless steel, C^{-2} clearly decrease with increasing pH. In this figure, the positive slopes in the main passive region are attributed to n-type behavior. According to Eq. (1), the donor density has been determined from the positive slopes in the main passive region [24–26]:

$$\frac{1}{C^2} = \frac{2}{\varepsilon\varepsilon_0 e N_D}\left(E - E_{FB} - \frac{kT}{e}\right) \quad \text{for n-type semiconductor} \quad (1)$$

where e is the electron charge, N_D is the donor density for n-type semiconductor (cm^{-3}), ε is the dielectric constant of the passive film (usually taken as 15.6), ε_0 is the vacuum permittivity, k is the Boltzmann constant, T is the absolute temperature and E_{FB} is the flat band potential. Fig. 4 shows the calculated donor densities for the passive films formed on AISI 430 ferritic stainless steel in NaOH solutions. The orders of magnitude are around 10^{21} cm^{-3} and are comparable to those reported in other studies [27]. According to Fig. 4, the donor density increases with pH. Based on PDM [19], the flux of oxygen vacancy and/or cation interstitials through the passive film is essential to the film growth process. In this concept, the dominant point defects in the passive film are considered to be oxygen vacancies and/or cation interstitials acting as electron donors.

3.3. *EIS measurements*

The EIS response of AISI 430 ferritic stainless steel in NaOH solutions with pH varying from 11.5 to 14.0 was performed and the results are presented as Nyquist and Bode plots in Fig. 5. For this stainless steel, the Nyquist and Bode plots show a resistive behavior at high frequencies, but in the middle to low frequency range there was a marked capacitive response. The Bode-phase curves show one time constant (only one maximum phase lag at the middle frequency range). The phase angle values remained very close to 80°. This evolution revealed the formation and growth of a passive film. Also, there was a decrease in low frequency impedance with increasing pH.

Based on these results, the equivalent circuit shown in Fig. 6 was used to simulate the measured impedance data of AISI 430 ferritic stainless steel in NaOH solutions with pH varying from 11.5 to 14.0. This equivalent circuit is composed of: R_s – solution resistance; Q_{pf} – constant phase element corresponding to the capacitance of the passive film; and R_{pf} – resistance of the passive film. This equivalent circuit has provided best fitting for the impedance data as shown in Fig. 5. This equivalent circuit composed by one time constant as

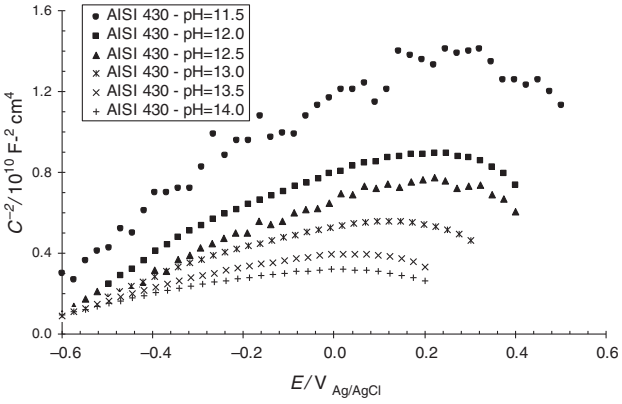

Fig. 3 – Mott–Schottky plots of AISI 430 stainless steel in NaOH solutions with pH varying from 11.5 to 14.0.

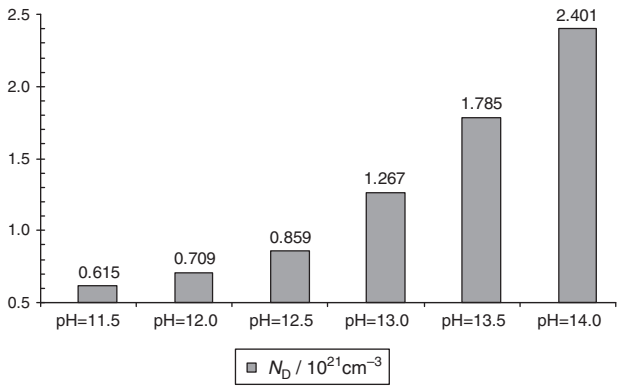

Fig. 4 – Effect of solution pH on the donor density of the passive films formed on AISI 430 stainless steel.

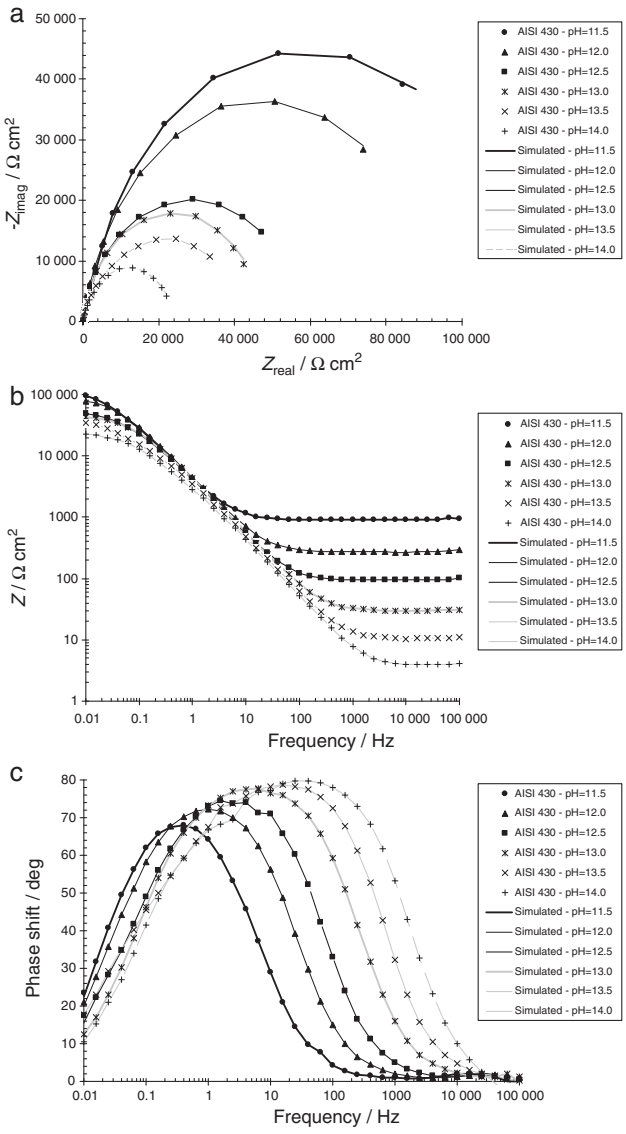

Fig. 5 – (a) Nyquist, (b) Bode and (c) Bode-phase plots of AISI 430 stainless steels in NaOH solutions with pH varying from 11.5 to 14.0.

proposed by Feng et al. [28,29] to describe the passive behavior of AISI 316L stainless steel in alkaline solutions. The impedance of the constant phase element is presented using Eq. (2):

$$Z_Q = [C(j\omega)^n]^{-1} \quad (2)$$

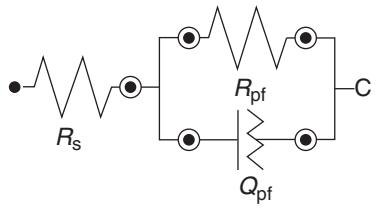

Fig. 6 – The best equivalent circuit tested to model the experimental EIS data with one time constant.

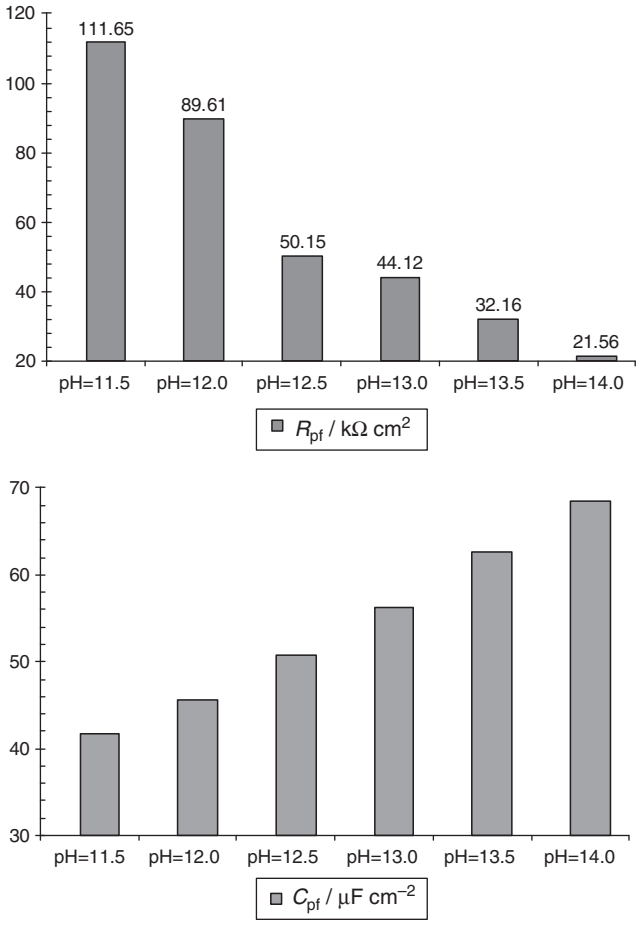

Fig. 7 – Effect of solution pH on the passive film resistance and passive film capacitance of AISI 430 stainless steel in NaOH solutions.

where n is associated with the roughness of the electrode surface [28,29]. Fig. 7 shows the effect of solution pH on the passive film resistance and capacitance of AISI 430 stainless steel. As can be seen in Fig. 7, for this stainless steel, passive film resistance decreases with increasing pH while passive film capacitance increases. According to the equivalent circuit shown in Fig. 6, the passive film thickness (d) can be calculated using Eq. (3) [30]:

$$d = \frac{\varepsilon\varepsilon_0}{C} \quad (3)$$

where C is the total capacitance of the passive film. Generally, a change in the total capacitance of the passive film can be used as an indicator for change in the passive film thickness. Therefore, the reciprocal capacitance of the passive film ($1/C$) is proportional to its thickness, which decreases with increasing pH.

Fig. 8 shows a linear relationship between the passive film thickness and the solution pH. As can be seen in Fig. 8, the calculated thickness ranges from about 0.132 nm at pH = 11.5 to 0.081 nm at pH = 14.0. These values of the thickness are considered to be eminently realistic [31]. It is clear that decreasing the solution pH give better conditions for forming the passive

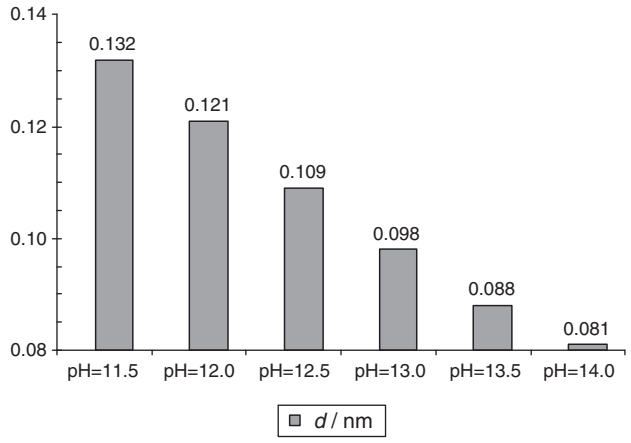

Fig. 8 – Effect of solution pH on the passive film thickness of AISI 430 stainless steel in NaOH solutions.

films with higher protection behavior, due to the growth of a much thicker and less defective passive films.

4. Conclusions

The effects of solution pH on the passivation behavior of the passive film formed on AISI 430 ferritic stainless steel at OCP in concentrated alkaline solutions were investigated in the present work. Conclusions drawn from the study are as follows:

1. Potentiodynamic polarization curves showed that the corrosion current density of AISI 430 stainless steel increased with increasing pH.
2. Mott–Schottky analysis revealed that passive films formed on AISI 430 stainless steel behave as n-type semiconductor and the donor density increased with increasing pH.
3. Nyquist and Bode plots show a resistive behavior at high frequencies, but in the middle to low frequency range, there was a marked capacitive response.
4. Bode-phase curves show one time constant (only one maximum phase lag at the middle frequency range). The phase angles values remained very close to 80°. This evolution revealed the formation and growth of a passive film.
5. EIS results showed that the reciprocal capacitance of the passive film decreased with increasing pH.
6. Also, EIS results showed that decreasing the solution pH offered better conditions for forming passive films with higher protection behavior, due to the growth of a much thicker and less defective film.

Conflict of interest

The authors declare no conflicts of interest.

REFERENCES

[1] Makkus RC, Janssen AHH, de Bruijn FA, Mallant RKAM. Stainless steel for cost-competitive bipolar plates in PEMFCs. Fuel Cells Bull 2000;3(17):5–9.
[2] Makkus RC, Janssen AHH, de Bruijn FA, Mallant RKAM. Use of stainless steel for cost competitive bipolar plates in the SPFC. J Power Sources 2000;86(1–2):274–82.
[3] Davies DP, Adcock PL, Turpin M, Rowen SJ. Stainless steel as a bipolar plate material for solid polymer fuel cells. J Power Sources 2000;86(1–2):237–42.
[4] Davies DP, Adcock PL, Turpin M, Rowen SJ. Bipolar plate materials for solid polymer fuel cells. J Appl Electrochem 2000;30(1):101–5.
[5] Wang H, Turner JA. Ferritic stainless steels as bipolar plate material for polymer electrolyte membrane fuel cells. J Power Sources 2004;128(2):193–200.
[6] Yang Y, Guo L, Liu H. Factors affecting corrosion behavior of SS316L as bipolar plate material in PEMFC cathode environments. Int J Hydrog Energy 2012;37(18):13822–8.
[7] Tian R, Sun J, Wang L. Plasma-nitrided austenitic stainless steel 316L as bipolar plate for PEMFC. Int J Hydrog Energy 2006;31(13):1874–8.
[8] Yang Y, Guo L-J, Liu H. Corrosion characteristics of SS316L as bipolar plate material in PEMFC cathode environments with different acidities. Int J Hydrog Energy 2011;36(2):1654–63.
[9] Feng K, Wu G, Li Z, Cai X, Chu PK. Corrosion behavior of SS316L in simulated and accelerated PEMFC environments. Int J Hydrog Energy 2011;36(20):13032–42.
[10] Kumagai M, Myung S-T, Asaishi R, Katada Y, Yashiro H. High nitrogen stainless steel as bipolar plates for proton exchange membrane fuel cells. J Power Sources 2008;185(2):815–21.
[11] Wind J, Späh R, Kaiser W, Böhm G. Metallic bipolar plates for PEM fuel cells. J Power Sources 2002;105(2):256–60.
[12] Kim KM, Kim JH, Lee YY, Kim KY. Effect of immersion in NaOH solution on ferritic stainless steel as a bipolar plate for polymer electrolyte membrane fuel cells. Int J Hydrog Energy 2011;36(20):13014–21.
[13] Lee S-J, Lai J-J, Huang C-H. Stainless steel bipolar plates. J Power Sources 2005;145(2):362–8.
[14] Kim KM, Kim KY. A new alloy design concept for austenitic stainless steel with tungsten modification for bipolar plate application in PEMFC. J Power Sources 2007;173(2):917–24.
[15] Addari D, Elsener B, Rossi A. Electrochemistry and surface chemistry of stainless steels in alkaline media simulating concrete pore solutions. Electrochim Acta 2008;53(27):8078–86.
[16] Chen YY, Liou YM, Shih HC. Stress corrosion cracking of type 321 stainless steels in simulated petrochemical process environments containing hydrogen sulfide and chloride. Mater Sci Eng A 2005;407(1–2):114–26.
[17] Hermas AA, Morad MS. A comparative study on the corrosion behaviour of 304 austenitic stainless steel in sulfamic and sulfuric acid solutions. Corros Sci 2008;50(9):2710–7.
[18] Sikora E, Macdonald DD. The passivity of iron in the presence of ethylenediaminetetraacetic acid I. General electrochemical behavior. J Electrochem Soc 2000;147(11):4087–92.
[19] Macdonald DD. On the tenuous nature of passivity and its role in the isolation of HLNW. J Nucl Mater 2008;379(1–3):24–32.
[20] Fattah-alhosseini A, Golozar MA, Saatchi A, Raeissi K. Effect of solution concentration on semiconducting properties of passive films formed on austenitic stainless steels. Corros Sci 2010;52(1):205–9.
[21] Amin MA, Mersal GA, Mohsen Q. Monitoring corrosion and corrosion control of low alloy ASTM A213 grade T22 boiler steel in HCl solutions. Arab J Chem 2011;4(2):223–9.
[22] Burstein GT. A hundred years of Tafel's equation: 1905–2005. Corros Sci 2005;47(12):2858–70.
[23] Lee S-J, Huang C-H, Chen Y-P. Investigation of PVD coating on corrosion resistance of metallic bipolar plates in PEM fuel cell. J Mater Process Technol 2003;140(1–3):688–93.

[24] Cheng YF, Yang C, Luo JL. Determination of the diffusivity of point defects in passive films on carbon steel. Thin Solid Films 2002;416(1–2):169–73.
[25] Li N, Li Y, Wang S, Wang F. Electrochemical corrosion behavior of nanocrystallized bulk 304 stainless steel. Electrochim Acta 2006;52(3):760–5.
[26] Escrivà-Cerdán C, Blasco-Tamarit E, García-García DM, García-Antón J, Guenbour A. Effect of potential formation on the electrochemical behaviour of a highly alloyed austenitic stainless steel in contaminated phosphoric acid at different temperatures. Electrochim Acta 2012;80:248–56.
[27] Oguzie EE, Li J, Liu Y, Chen D, Li Y, Yang K, et al. The effect of Cu addition on the electrochemical corrosion and passivation behavior of stainless steels. Electrochim Acta 2010;55(17):5028–35.
[28] Feng Z, Cheng X, Dong C, Xu L, Li X. Effects of dissolved oxygen on electrochemical and semiconductor properties of 316L stainless steel. J Nucl Mater 2010;407(3):171–7.
[29] Feng Z, Cheng X, Dong C, Xu L, Li X. Passivity of 316L stainless steel in borate buffer solution studied by Mott–Schottky analysis, atomic absorption spectrometry and X-ray photoelectron spectroscopy. Corros Sci 2010;52(11):3646–53.
[30] Luo H, Dong CF, Li XG, Xiao K. The electrochemical behaviour of 2205 duplex stainless steel in alkaline solutions with different pH in the presence of chloride. Electrochim Acta 2012;64:211–20.
[31] Olsson COA, Landolt D. Passive films on stainless steels – chemistry, structure and growth. Electrochim Acta 2003;48(9):1093–104.